

Evolution of galaxies: observational evidences

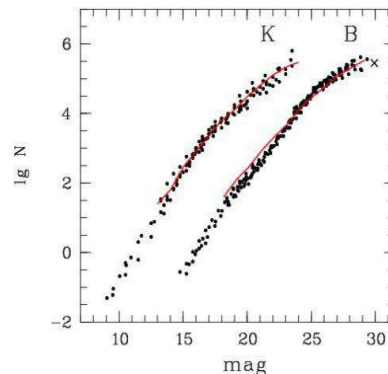
Galaxy counts

Over many years, galaxy counts, i.e., the plot of the observed number of galaxies at the limiting magnitude, have been considered to be an important cosmological test. In particular, in the 1930s, Hubble tried to apply them to estimate the curvature of space.

It became clear later that practical application of this test is so difficult (photometric errors, the account for k -correction, the evolution of galaxies with time) that “any attempt to do so appears to be a waste of telescope time” (Sandage 1961). Presently, deep counts are regarded not as a cosmological test but rather as a test of galaxy formation and evolution.

Galaxy counts

Figure summarizes modern results of differential galaxy counts. (Only data obtained after 1995 are shown.) With each filter, the results of about twenty projects (including 2MASS, SDSS, HDF, CDF, NDF, etc.) are summarized; with filter B , counts in the SDF, VVDS, and HUDF fields are added.



Galaxy counts

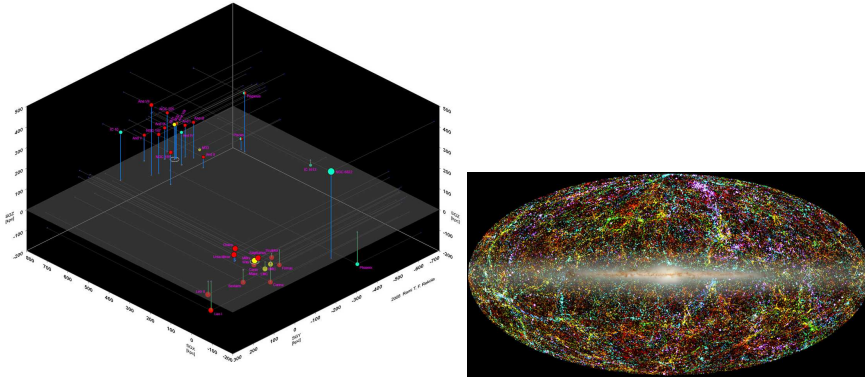
Main result:

good agreement between the results of different works. For example, for $B \approx 25^m$, the count dispersion is only about 10% (accounting for the photometry, different selection of galaxies, etc., this dispersion must be even smaller), which clearly illustrates the homogeneity and isotropy of large-scale galaxy distribution.

The solid lines in the figure show predictions of a semianalytic model of galaxy formation (Nagashima et al. 2002). However, the model predictions are not fully definitive due to many parameters characterizing galactic properties and their evolution with z (including spatial density evolution). For further progress in this field, both observational data and theoretical understanding of galaxy evolution must be improved.

Galaxy distribution

The distribution of galaxies in the nearby volume of the Universe is highly inhomogeneous. When passing to the hundred Megaparsec scale, the density fluctuations smoothen and the distribution becomes more homogeneous.



Galaxy distribution

Galaxies tend to cluster. This means that the probability of finding a galaxy at some point P is highest when P is known to be close to another galaxy. We saw a hint of this in the Local Group because there are 2 big galaxies, not one.

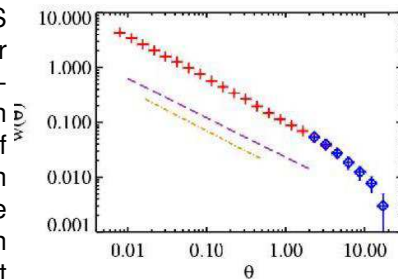
The clustering of galaxies is usually described in terms of two-point correlation functions $\xi(r)$ and $\omega(\theta)$. The former function describes the joint probability of finding two galaxies separated by a distance r , and the latter characterizes the joint probability of detecting two objects at the angular distance θ . To calculate $\xi(r)$, spatial distances between galaxies should be known, and in practice it is therefore more convenient to measure the (angular) two-point correlation function $\omega(\theta)$.



Galaxy distribution

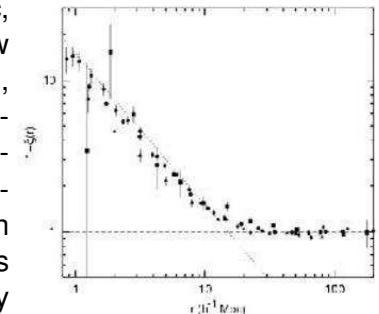
From $\omega(\theta)$, one can then estimate $\xi(r)$ because both functions are related through the Limber integral equation. If $\xi(r)$ can be represented as a power law $\xi(r) = (r/r_0)^{-\gamma}$, the angular correlation also takes a power-law form $\omega(\theta) \propto \theta^{1-\gamma}$.

The angular correlation function for ~ 0.5 million galaxies from the 2MASS survey (+APM, SDSS). At angular scales $1' < \theta < 2.05'$, this function is well fit by a power law with $1 - \gamma = -0.79 \pm 0.02$. The amplitude of $\omega(\theta)$ depends on the sample depth – for brighter and closer objects, the clustering amplitude increases (this, in particular, explains the systematic shift between different survey data).



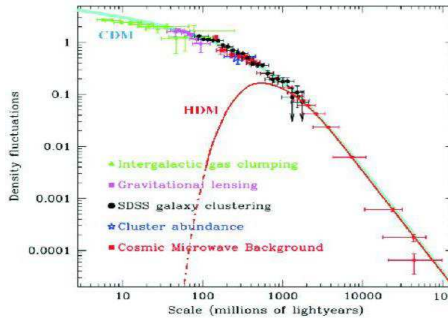
Galaxy distribution

The spatial correlation function $\xi(r)$ calculated in different papers. In the range $0.1 \text{ Mpc} \leq r \leq 20 \text{ Mpc}$, this function follows a power law with the exponent $\gamma \approx 1.7 - 1.8$, and then tends to zero. The characteristic clustering scale (correlation length) r_0 for nearby galaxies is $\sim 5-7 \text{ Mpc}$. The correlation length depends on the properties of galaxies, such as their luminosity and morphological type, but is independent of the sample depth.



Galaxy distribution

Modern survey data allow determining the density fluctuations in the Universe as a function of the scale of averaging. (The power spectrum of the SDSS galaxies, which has been used to plot this figure, is based on data on $2 \cdot 10^5$ galaxies.) Figure shows that different kinds of data, from galaxy density fluctuations to cosmic microwave background anisotropy, form a unique smooth dependence described by the CDM model.



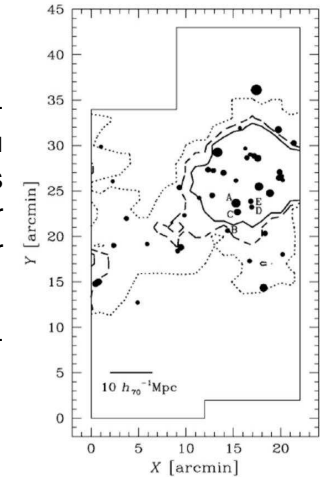
Navigation icons: back, forward, search, etc.

Galaxy distribution

Examples of large-scale structure at high redshifts - LAEs

Sky distribution of 43 LAE candidates at $z = 4.86$ (Shimasaku et al. 2003). LAE candidates are shown by circles. Brighter candidates are shown by larger circles.

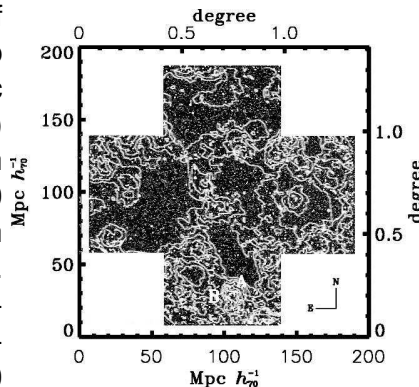
Progenitor of a cluster of galaxies?



Navigation icons: back, forward, search, etc.

Galaxy distribution

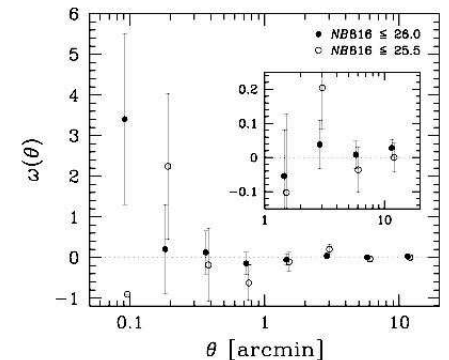
Ouchi et al. (2005) carried out extensive deep narrowband imaging in the 1 sq.deg. sky of the Subaru/XMM-Newton Deep Field and obtained a cosmic map of 515 Ly α emitters (LAEs) at $z \approx 5.7$ in a volume with a transverse dimension of 180 Mpc \times 180 Mpc and a depth of ~ 40 Mpc in comoving units. This cosmic map shows filamentary LSSs, including clusters and surrounding 10–40 Mpc scale voids, similar to the present-day LSSs.



Navigation icons: back, forward, search, etc.

Galaxy distribution

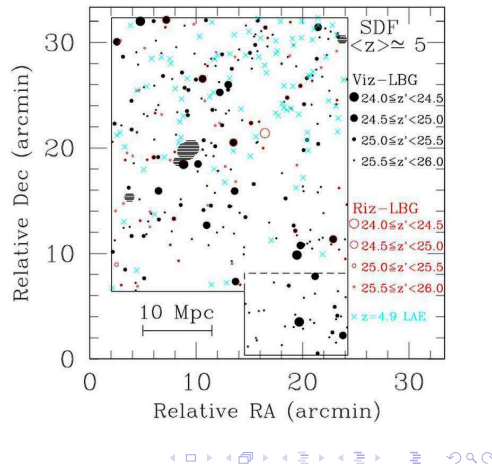
Shimasaku et al. (2006): angular correlation function of LAEs at $z = 5.7$. The filled and open circles correspond to the whole sample ($N = 89$) and a bright sample ($N = 53$), respectively.



Navigation icons: back, forward, search, etc.

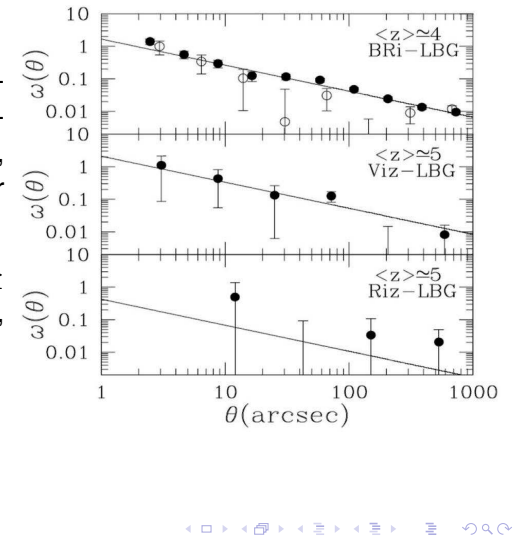
Examples of large-scale structure at high redshifts - LBGs

Ouchi et al. (2004): sky distributions of $z \sim 5$ LBGs detected in the SDF.



Ouchi et al. (2004) calculated angular two-point correlation functions of LBGs, and found clear signals for LBGs at $z = 4$ and 5 .

The correlation length of $L \geq L^*$ LBGs is almost constant, ~ 7 Mpc, over $z \sim 3 - 5$.



Correlation length and galaxy-dark matter bias as a function of redshift.

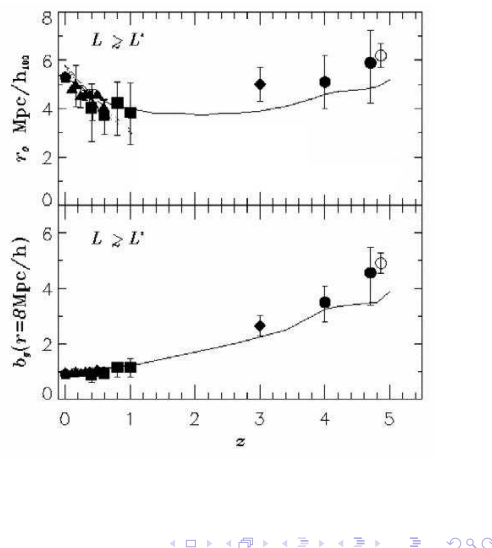
A bias factor b is defined by

$$\xi(r)_{\text{galaxies}} = b^2 \xi(r)_{\text{mass}},$$

or

$$b^2 = \sigma_8^2(\text{galaxies}) / \sigma_8^2(\text{mass}).$$

($b \neq 1$ - light does not follow mass.)



The luminosity function (LF) is the dependence of the number of galaxies within a unit volume on their luminosity. It is one of the most important integral characteristics of galaxies. The LF allows estimating the mean luminosity density in the Universe. The LF form is one of the main tests of galaxy formation models.

The standard form of the LF is the so-called Schechter function

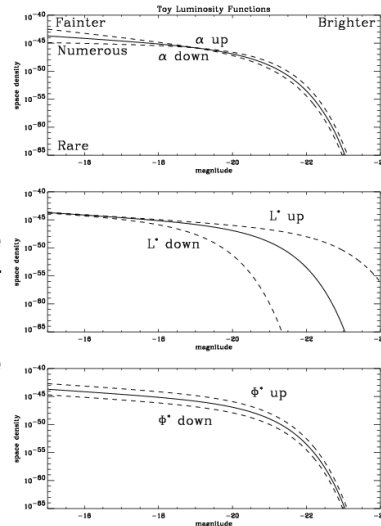
$$\phi(L)dL = \phi_* (L/L_*)^\alpha \exp(-L/L_*) d(L/L_*),$$

where $\phi(L)dL$ is the number of galaxies with the luminosity from L to $L + dL$ per unit volume, and ϕ_* , L_* and α are parameters.

⌞ Luminosity function evolution

The parameter ϕ_* yields the normalization of the LF, L_* is the characteristic luminosity, and α determines the slope of the weak wing ($L < L_*$) of the LF: the weak wing of the LF is flat for $\alpha = -1$, the LF increases with decreasing L for $\alpha < -1$, and decreases at $\alpha > -1$.

The Schechter function fits well the real LF of field galaxies and clusters and has convenient analytical properties.



Navigation icons: back, forward, search, etc.

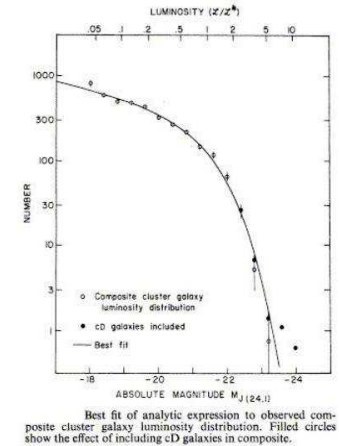
⌞ Luminosity function evolution

The luminosity density of galaxies is

$$\begin{aligned} \rho_L &= \int_0^\infty L \phi(L) dL = \\ &= L_* \int_0^\infty y \phi(y) dy = \\ &= L_* \phi_* \int_0^\infty y^{1+\alpha} e^{-y} dy = \\ &= L_* \phi_* \Gamma(\alpha + 2) \end{aligned}$$

and the galaxy density is

$$\rho = \rho_L / L_* = \phi_* \Gamma(\alpha + 2).$$



Best fit of analytic expression to observed composite cluster galaxy luminosity distribution. Filled circles show the effect of including cD galaxies in composite.

Navigation icons: back, forward, search, etc.

⌞ Luminosity function evolution

The local LF of galaxies is relatively well studied. According to many projects (including the 2dF and SDSS surveys), within the luminosity range $-15^m \leq M(B) \leq -22^m$, the LF can be described with the following values of parameters:

$$\begin{aligned} \alpha &\approx -(1.1 - 1.2), \\ M_*(B) &\approx -20.^m2 \quad (L_*(B) = 1.9 \cdot 10^{10} L_{\odot,B}), \text{ and} \\ \phi_* &\approx (0.5 - 0.7) \cdot 10^{-2} \text{ Mpc}^{-3}. \end{aligned}$$

Therefore, the luminosity density of galaxies at $z = 0$ is

$$\rho_L(B) = \phi_* L_* \Gamma(\alpha + 2) \approx 1.3 \cdot 10^8 L_{\odot,B} / \text{Mpc}^3$$

and the galaxy density is

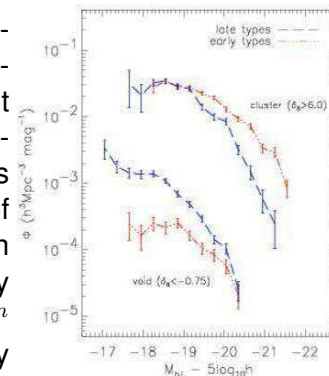
$$\rho = \rho_L / L_* = \phi_* \Gamma(\alpha + 2) \sim 10^{-2} \text{ Mpc}^{-3}.$$

The LF of local galaxies depends on their morphological type and environment.

Navigation icons: back, forward, search, etc.

⌞ Luminosity function evolution

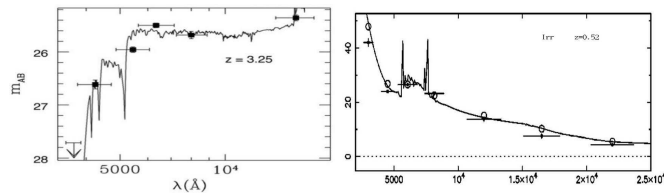
Croton et al. (2005): direct comparison of the early- and late-type galaxy populations in the cluster environment and void regions of the 2dF survey. The void population is composed almost exclusively of faint late-type galaxies, while in the cluster regions the galaxy population brighter than -19^m consists predominantly of early types.



Navigation icons: back, forward, search, etc.

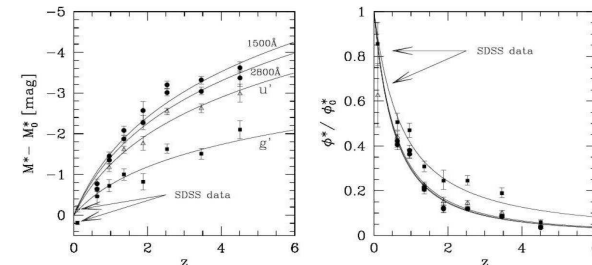
└ Luminosity function evolution

Numerous deep field studies performed over the last ten years have enabled the evolution of the LF with z to be determined. In solving this problem, the so-called 'photometric redshifts' inferred from multicolor photometry are used instead of spectroscopic ones for the most distant objects. Such a photometry allows a kind of a low-resolution spectrum and hence z of an object to be obtained. Photometric estimations of z are being made with $\approx 10\%$ – 20% accuracy, which is quite sufficient to derive the LF for large samples of galaxies.



└ Luminosity function evolution

Observations suggest a differential (depending on the galaxy type and the color band) evolution of the LF. Different papers give somewhat different results, but the qualitative picture emerging is as follows: the value of M_* increases with z , while ϕ_* decreases. The evolution of the LF slope is much less definitive.



└ Luminosity function evolution

By considering different types of objects separately, the space density of elliptical and early spiral galaxies almost stays constant or slightly decreases toward $z \sim 1$, while their LF evolution can be described as a change in the luminosity of galaxies (they become brighter). In contrast, the space density of late spiral galaxies with active star formations notably increases toward $z \sim 1$.

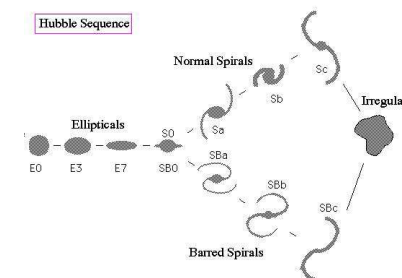
The change in the LF of galaxies alters the luminosity density they produce: from $z = 0$ to $z \sim 3$, the value of ρ_L increases, with the strongest growth being in the UV region (by about 5 times).



└ Evolution of the galaxy structure

└ Morphological evolution

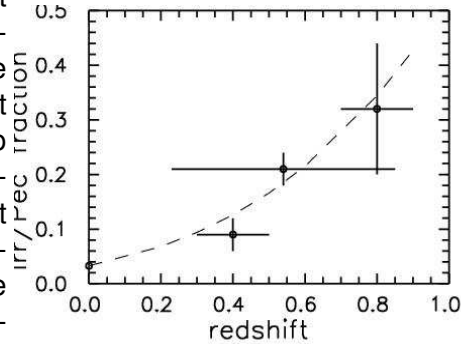
One of the main goals of the deep field galaxy studies is the origin and evolution of the Hubble sequence. In the local Universe, the optical morphology of the vast majority of bright galaxies can be described in terms of a simple classification scheme suggested by Hubble. Only about 5% of nearby objects do not fit this scheme and are related to irregular or interacting galaxies.



Evolution of the galaxy structure

↳ Morphological evolution

The deep HST fields for the first time allowed us to see the structure of distant galaxies. The very first studies revealed that the fraction of galaxies that do not fit the Hubble scheme increases for fainter objects. At $z \sim 1$ (where the age of the Universe is about half the Hubble time), the fraction of such galaxies reaches 30%–40%.



◀ ▶ ⏪ ⏩ 🔍 🔄

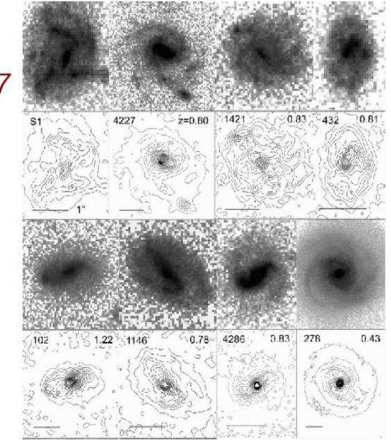
Evolution of the galaxy structure

↳ Morphological evolution

Bar fraction

Abraham et al. (1999): decline in the rest-frame optical bar fraction from ~24% at $z \sim 0.2-0.7$ to below 5% at $z > 0.7$.

Elmegreen et al. (2004), Jogee et al. (2004)... : optical fraction of strong bars remains at ~30% from the present to $z \sim 1$.



◀ ▶ ⏪ ⏩ 🔍 🔄

Evolution of the galaxy structure

↳ Morphological evolution

Fraction of interacting and merging galaxies

The statistics of objects in some deep fields also suggests that the fraction of interacting galaxies and merging galaxies increases with z . With the $(1+z)^m$ growth assumed, observational data suggest $m \approx 2-4$ for $z \sim 1$. The evolution of the merging rate is likely to depend on the mass of galaxies – it is most pronounced for massive objects.

It is much more difficult to draw definitive conclusions on the structure evolution for objects at $z \geq 1$ due to the increasing effects of the k -correction, the cosmological dimming of surface brightness and degradation of the resolution.

◀ ▶ ⏪ ⏩ 🔍 🔄

Evolution of the galaxy structure

↳ Morphological evolution

Kartaltepe et al. (2007):

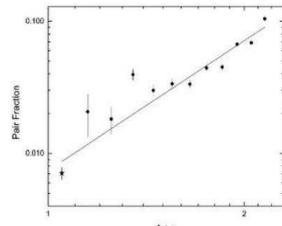
Reference	mag ^a	z^b	z Range ^c	Sample Size ^d	#P or M ^e	m or n^f
<i>Galaxy Pair Fraction Studies</i>						
Zepf & Koo (1989)	$B \leq 22$	A	$\langle z \rangle = 0.25$	~ 1000	20	4.0 ± 2.5
Carlberg et al. (1994)	$V \leq 22.5$	S	$\langle z \rangle = 0.42$	1062	14	2.3 ± 1.0
Burkey et al. (1994)	$I = 18.5-23$	A,S	0.4 – 0.7	146	50	3.5 ± 0.5
Woods et al. (1995)	$I \leq 24$	N	...	~ 1000	23	0
Neuschaefer et al. (1995)	$I \leq 22$...	$z_{med} = 0.5$	~ 4500	...	0
Yee & Ellingson (1995)	$r \leq 21.5$	S	$\langle z \rangle = 0.38$	107	25	4.0 ± 1.5
Neuschaefer et al. (1997)	$I = 18-23$	S	$\lesssim 1-2$	~ 22400	90	1.2 ± 0.4
Patton et al. (1997)	$r \leq 22$	S	$\langle z \rangle = 0.33$	545	73	2.8 ± 0.9
Wu & Keel (1998)	$I \leq 24$	A	~ 2	...	10	0 – 2
Carlberg et al. (2000)	$M_R \leq 19.8$	S	0.1 – 1.1	~ 3300	109	0.1 ± 0.5^g
Le Fevre et al. (2000)	$\delta m \leq 1.5$	S	≤ 1	285	26	2.7 ± 0.6
Patton et al. (2002)	$R_c \leq 21.5$	S	0.12 – 0.55	4184	88	2.3 ± 0.7^g
Lin et al. (2004)	$M_B = (21-19)$	S	0.45 – 1.2	5000	...	1.60 ± 0.29
Lin et al. (2004)					...	0.51 ± 0.28^g
This work^h	$> L_V^*$	Ph	0 – 1.2	106118	1749	3.1 ± 0.1
<i>Morphologically Selected Merger Studies</i>						
Le Fevre et al. (2000)	$\delta m \leq 1.5$	S	≤ 1	285	49	3.4 ± 0.6
Reshetnikov (2000)	...	Ph	0.5 – 1.0	...	14	$3.6^{+1.2}_{-0.9}$
Conselice et al. (2003)	$M_B \leq -18$	Ph,S	0 – 3	1212	43	4 – 6
Lavery et al. (2004)	...	Ph,S	0.1 – 1.0	...	25	5.2 ± 0.7
Lotz et al. (2006)	$> 0.4L_B^*$	S	0.2 – 1.2	2368	157	1.12 ± 0.60^g

◀ ▶ ⏪ ⏩ 🔍 🔄

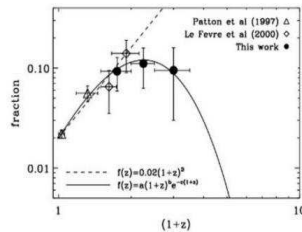
Evolution of the galaxy structure

Morphological evolution

Frequency of luminous galaxy pairs (Kartaltepe et al. 2007)



$m = 3.1 \pm 0.1$ - solid line



Galaxy merger fraction (Ryan et al. 2008)



Evolution of the galaxy structure

Morphological evolution

Abraham & van den Bergh (2001):

Table 1: Summary of key ages in galaxy morphology to $z=1$

Redshift	Look-back Time	Key Developments in Galaxy Morphology
$z < 0.3$	$< \sim 3.5$ Gyr	Grand-design spirals exist. Hubble scheme applies in full detail.
$z \sim 0.5$	~ 5 Gyr	Barred spirals become rare. Spiral arms are underdeveloped. The bifurcated "tines" of the Hubble tuning fork begin to evaporate.
$z > 0.6$	> 6 Gyr	Fraction of mergers and peculiar galaxies increases rapidly. By $z=1$ around 30% of luminous galaxies are off the Hubble sequence.

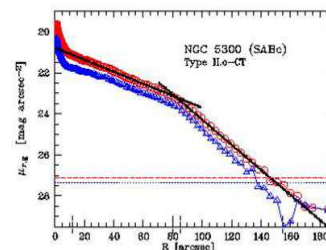


Evolution of the galaxy structure

Radial surface brightness of spiral galaxies

Trujillo & Pohlen (2005): 36 HUDF galaxies ($0.1 < z < 1.1$), 21 with downbending disks

Trujillo & Pohlen (2005) used the position of the truncation (break radius) as a direct estimator of the size of the stellar disk.



They found that the radial position of the truncations has increased with cosmic time by 1-3 kpc since $z \sim 1$.

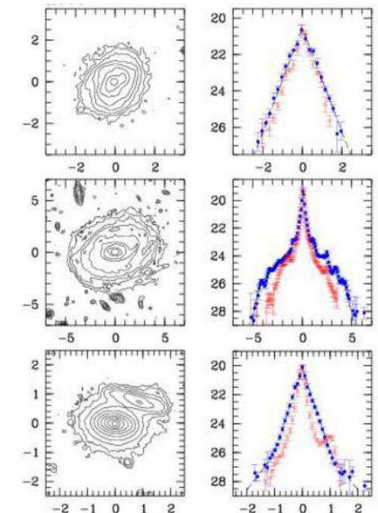


Evolution of the galaxy structure

Radial surface brightness of spiral galaxies

Sample: all objects with $V_{606} < 23.5^m$ and $b/a > 0.4$ in the HDF-N, HDF-S and HUDF

$N=201$ object:
29 stars,
123 spirals with $b/a > 0.4$
(117 with z)



Evolution of the galaxy structure

Radial surface brightness of spiral galaxies

General characteristics of the sample (117 galaxies) are

$\langle M_B \rangle = -19.46 \pm 1.58$ (mean absolute magnitude),

$\langle z \rangle = 0.53 \pm 0.27$ (mean redshift),

Frequency of exp. profiles – 0.38 ± 0.06 (N=44),

downbending profiles – 0.25 ± 0.05 (N=29),

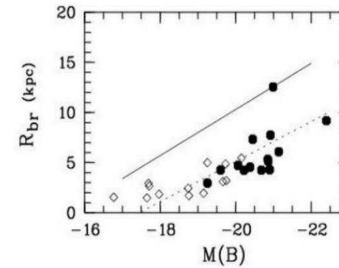
upbending profiles – 0.16 ± 0.04 (N=19),

peculiar surf. brightness – 0.21 ± 0.04 (N=25).

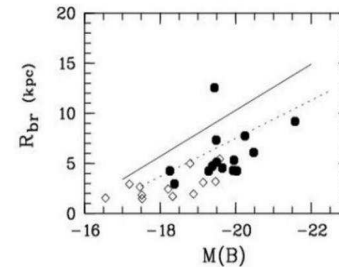
Navigation icons

Evolution of the galaxy structure

Radial surface brightness of spiral galaxies



Observed relation between the truncation radius and absolute magnitude in the rest-frame B band. Filled circles – galaxies with $z \geq 0.45$, rhombs – $z < 0.45$ galaxies.



The same relation after correcting M_B values for the luminosity evolution. Solid line represents the local relation (Trujillo and Pohlen 2005), dotted lines – relations for distant spirals from the same work.

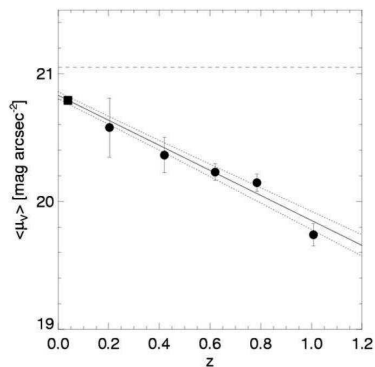
Navigation icons

Evolution of the galaxy structure

Radial surface brightness of spiral galaxies

Surface brightness

Barden et al. (2005): strong evolution in the magnitude-size scaling relation for galaxies with $M_V \leq -20^m$, corresponding to a brightening of $\Delta\mu(V) \sim 1$ in rest-frame V band by $z \sim 1$.



Navigation icons

Evolution of the galaxy structure

Vertical surface brightness distribution

Reshetnikov, Battaner, Combes, Jimenez-Vicente (2002), Reshetnikov, Dettmar, Combes (2003)

Sample: 45 edge-on galaxies in the HDF-N and HDF-S with $d > 1.3''$

Mean characteristics: $\langle I_{814} \rangle = 24.4 \pm 1.2$

$\langle b/a \rangle = 0.32 \pm 0.08$

$\langle z \rangle = 0.89 \pm 0.44$

$\langle M(B) \rangle = -18^m \pm 1.3$

Navigation icons

Evolution of the galaxy structure

Vertical surface brightness distribution

Can we resolve edge-on galaxies?

Mean minor axis of our sample edge-on galaxies is $0.7''$ or 5 PSF.

Mean corrected vertical scale is
 $\langle h_z \rangle = 0.46 \pm 0.21 \text{ kpc}$
 or
 $\langle z_0 \rangle = 0.9 \text{ kpc}$

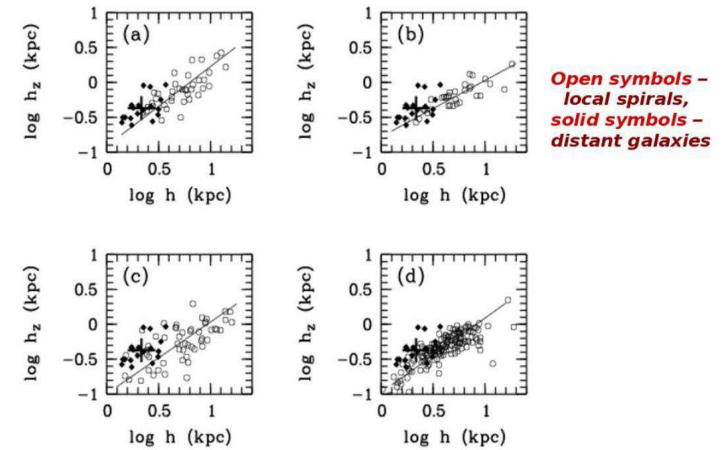
$\langle h / h_z \rangle = 5.4 \pm 2.0$ (19 exp disks)

Local galaxies ~ 10

Navigation icons

Evolution of the galaxy structure

Vertical surface brightness distribution



$z \sim 1$ disks are definitely thicker in comparison to local galaxies (by factor 1.5-2) (+ Elmegreen & Elmegreen 2006)

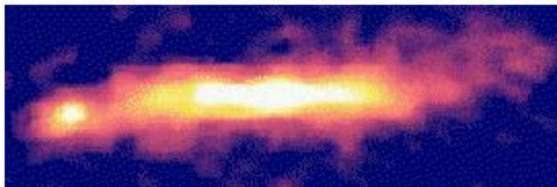
Navigation icons

Evolution of the galaxy structure

Vertical surface brightness distribution

Distant warps

9 of 45 galaxies show integral-like warp (20%) with mean amplitude $\sim 6^\circ$

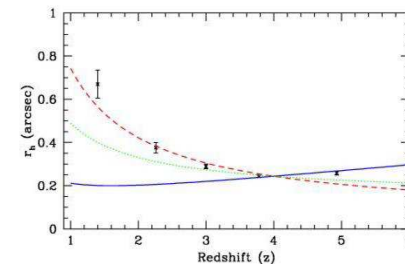


Almost all galaxy disks at $z \sim 1$ might be warped!
 Fraction of strong warps ($> 4.5^\circ$) changes as $(1+z)^4$

Navigation icons

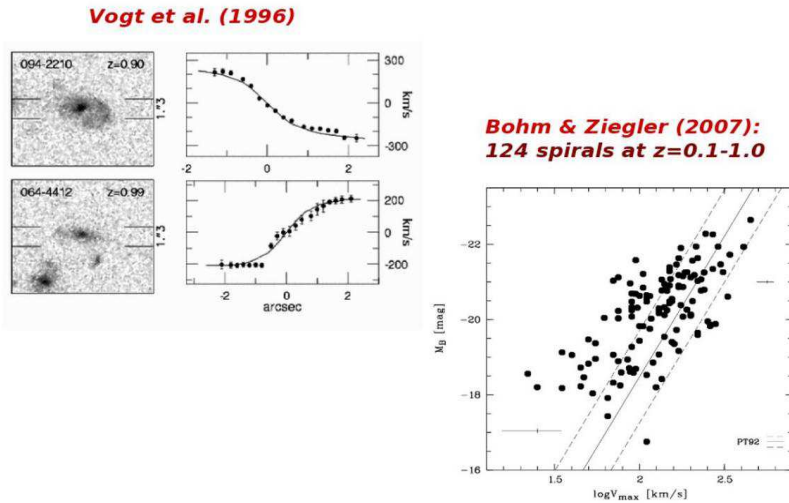
Sizes of galaxies

Ferguson et al. (2004): half-light radii vs. redshift (GOODS projects).
 The solid blue curve shows the expected trend if physical sizes do not evolve. The dashed red curve shows the trend if sizes evolve as $H^{-1}(z)$.



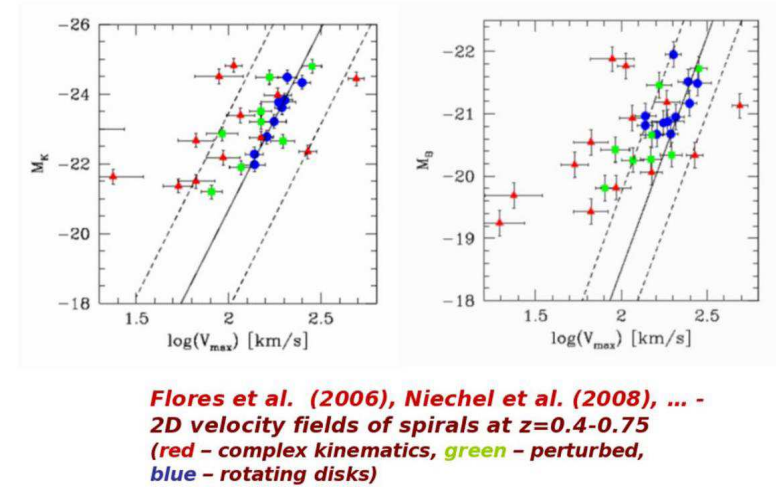
Navigation icons

⊥ Kinematics of distant spirals



◀ ▶ ⏪ ⏩ 🔍 ↺

⊥ Kinematics of distant spirals



◀ ▶ ⏪ ⏩ 🔍 ↺

⊥ Kinematics of distant spirals

Flores et al. (2006), Yang et al. (2007), Niechel et al. (2008), Puech et al. (2008) - 2D velocity fields of 65 spirals at z=0.4-0.75 (ESO-VLT)

Main conclusions:

At z~0.6, almost 40% of all galaxies are not rotating disks (not at dynamical equilibrium)

The zero point of the TF relation (K-band) evolve (~0.7^m brightening between z=0 and z~0.6)

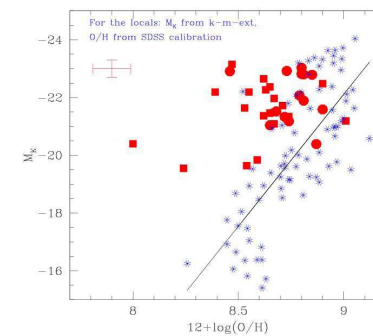
Galaxy kinematics are evolving very rapidly!

◀ ▶ ⏪ ⏩ 🔍 ↺

⊥ Chemical evolution

Example: M_K -metallicity relation for the intermediate- z ($z = 0.4 - 1$) starburst galaxies (red symbols) and local spirals (blue stars) – Liang et al. (2005).

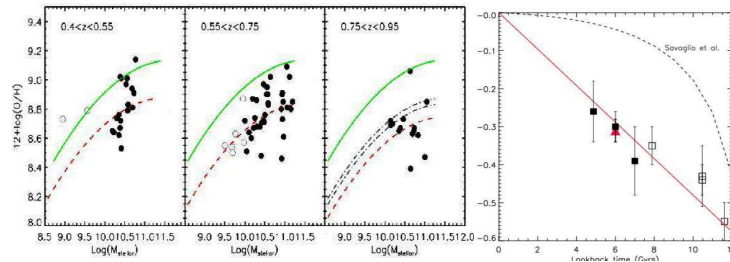
(The oxygen abundances are derived from $R_{23} = [OII]\lambda 3727/H\beta + [OIII]\lambda 4959, 5007/H\beta$.)



◀ ▶ ⏪ ⏩ 🔍 ↺

Chemical evolution

Rodrigues et al. (2008):

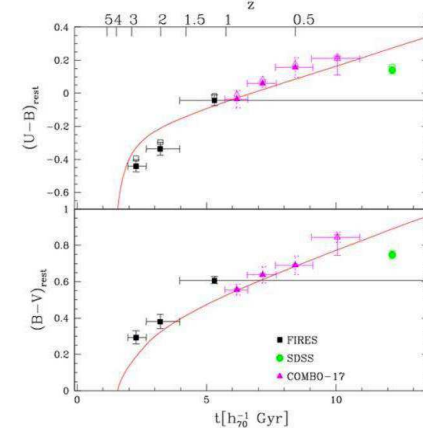


Conclusions: The predominant population of $z \sim 0.6$ starbursts and luminous IR galaxies (LIRGs) are on average, two times less metal rich than the local galaxies at a given stellar mass; the metal abundance of the gaseous phase of galaxies is evolving linearly with time, from $z = 1$ to $z = 0$ and after comparing with other studies, from $z = 3$ to $z = 0$.

Navigation icons

Optical colors

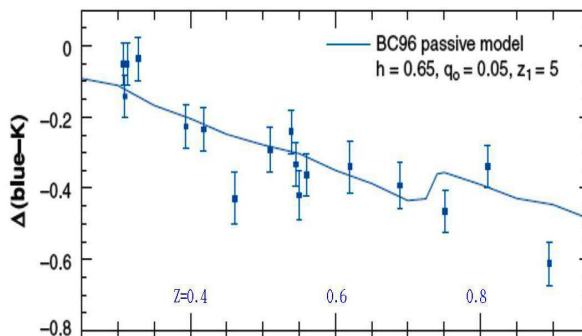
Rudnick et al. (2003): the cosmic rest-frame color of all the visible stars that lie in galaxies with $L_V > 1.4 \times 10^{10} L_\odot$. (Solid lines – a model with an exponentially declining SFH with $\tau = 6$ Gyr and $z_{start} = 4.0$.)



Navigation icons

Optical colors

The color evolution of early-type galaxies in clusters out to $z \approx 0.9$ (blue curve – purely passive evolution model).



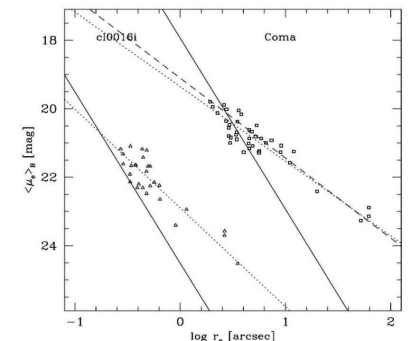
Navigation icons

Fundamental plane evolution

Kormendy relation

Ziegler et al. (1999): KR for distant galaxy clusters ($z = 0.4 - 0.55$).

An average brightening of distant ellipticals by $0.^m42$ at $z = 0.4$ and $0.^m73$ at $z = 0.55$. The luminosity evolution of early-type galaxies since intermediate redshifts as derived from the Kormendy relations is compatible with passive evolution models.



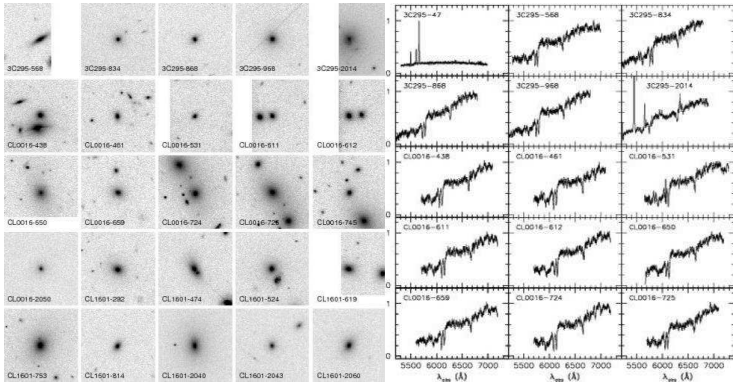
The (observed) Kormendy relation (dotted lines) for the distant cluster sample *c100161* (triangles) compared with the local sample (squares). The solid line represents the magnitude limit, which is shifted to the Coma SBD sample according to the calculated distance modulus and the expected luminosity evolution. The dashed line is the fit to this reduced sample.

Navigation icons

⊥ Fundamental plane evolution

Fundamental plane

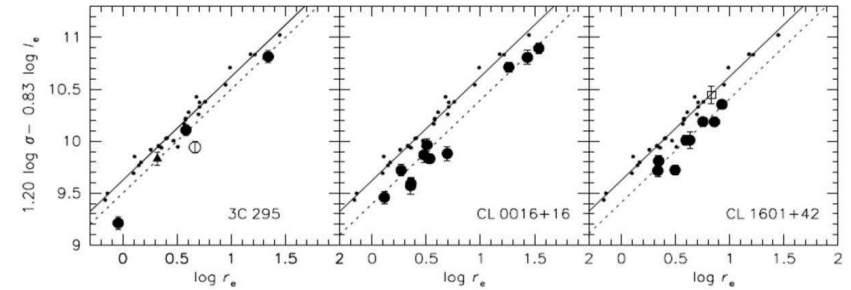
van Dokkum & van der Marel (2007): new spatially-resolved Keck spectroscopy of early-type galaxies in three galaxy clusters at $z \approx 0.5$.



Navigation icons: back, forward, search, etc.

⊥ Fundamental plane evolution

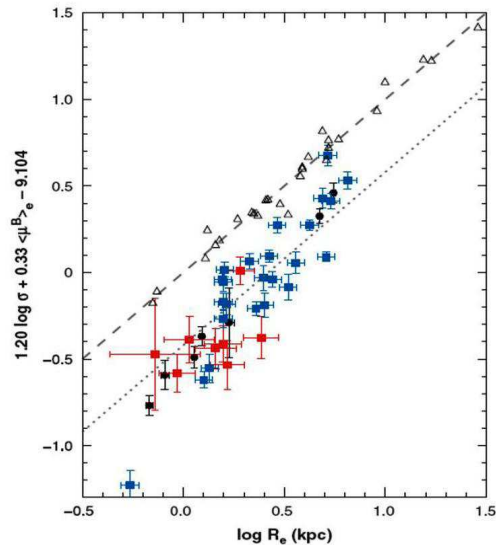
Edge-on projection of the FP in the three clusters. Dots are galaxies in the nearby Coma cluster. The solid line is a fit to Coma.



3C 295 - $z = 0.46$, CL 0016+16 - $z = 0.55$, CL 1601+42 - $z = 0.42$.

Navigation icons: back, forward, search, etc.

⊥ Fundamental plane evolution



An edge-on view of the fundamental plane for field early-type galaxies at $z \sim 1.1$ from di Serego Alighieri et al. (2005, red squares and black circles) and Treu et al. (2005b, blue squares). Open triangles refer to the Coma ellipticals from Jørgensen, Franx & Kjaergaard (1995) and the dashed line is a best fit to the data. The dotted line is shifted parallel to the dashed line by an amount in surface brightness corresponding to the observed shift of the fundamental plane of galaxy clusters (i.e., $\Delta M/L_B = -0.46z$, van Dokkum & Stanford 2003). The effective surface brightness in the B band (μ_B) is in magnitudes per arcsec².

Navigation icons: back, forward, search, etc.

⊥ Fundamental plane evolution

Evolution of the zeropoint of the FP can be interpreted as a systematic change of the mean M/L ratio with redshift. The conversion of zeropoint offsets to offsets in M/L ratio assumes that early-type galaxies form a homologous family and that the FP is a manifestation of an underlying relation between the M/L ratio of galaxies and other parameters.

Starting from the empirical FP relation and assuming $M \propto \sigma^2 r_e$ and $L \propto I_e r_e^2$, this underlying relation is

$$M/L \propto \sigma^{2+a} r_e^{-(1+b)/b}$$

Navigation icons: back, forward, search, etc.

↳ Fundamental plane evolution

Evolution of the mean M/L_B ratio of field galaxies with $M > 10^{11} M_\odot$ (blue symbols) compared to that of cluster galaxies (red symbols). The age difference between massive field ($z_f = 1.95$) and cluster ($z_c = 2.23$) galaxies is small at $\sim 4\%$.

